CHEMICAL ENGINEERING RESEARCH AND DESIGN XXX (2014) XXX–XXX

Contents lists available at ScienceDirect

Chemical Engineering Research and Design

journal homepage: www.elsevier.com/locate/cherd

Diffusional mass transfer model for the adsorption of food dyes on chitosan films

G.L. Dotto[a,*], C. Buriol[b], L.A.A. Pinto[c]

[a] Chemical Engineering Department, Federal University of Santa Maria – UFSM, 1000 Roraima Avenue, 97105-900 Santa Maria, RS, Brazil

[b] Mathematical Department, Federal University of Santa Maria – UFSM, 1000 Roraima Avenue, 97105-900 Santa Maria, RS, Brazil

[c] Unit Operation Laboratory, School of Chemistry and Food, Federal University of Rio Grande – FURG, 475 Engenheiro Alfredo Huch Street, 96203-900 Rio Grande, RS, Brazil

ABSTRACT

The adsorption kinetics of erythrosine B and indigo carmine on chitosan films was studied by a diffusional mass transfer model. The experimental curves were obtained in batch system under different conditions of stirring rate (80–200 rpm) and initial dye concentration (20–100 mg L^{-1}). For the model development, external mass transfer and intraparticle diffusion steps were considered and the specific simplifications were based on the system characteristics. The proposed diffusional mass transfer model agreed very well with the experimental curves, indicating that the surface diffusion was the rate limiting step. The external mass transfer coefficient (k_f) was dependent of the operating conditions and ranged from 1.32×10^{-4} to 2.17×10^{-4} m s^{-1}. The values of surface diffusion coefficient (D_s) increased with the initial dye concentration and were in the range from 0.41×10^{-14} to 22.90×10^{-14} m^2 s^{-1}. The Biot number ranged from 17.0 to 478.5, confirming that the intraparticle diffusion due to surface diffusion was the rate limiting step in the adsorption of erythrosine B and indigo carmine on chitosan films.

Keywords: Biot; Chitosan films; Dyes; Diffusional model; External mass transfer; Surface diffusion

1. Introduction

Synthetic dyes, such as, erythrosine B and indigo carmine are extensively used in food processing industry to confer, intensify and restore the color of the final products (Downham and Collins, 2000). A portion of these dyes is lost during the manufacturing and processing operations, and as consequence, a considerable amount of dye–containing effluents is generated (Gupta and Ali, 2013). As reported in recent studies, the dye-containing effluents have negative direct and indirect impacts on human health and the environment, and should be carefully treated before discharge (Gupta and Suhas, 2009; Srinivasan and Viraraghavan, 2010; Verma et al., 2012). Several methods have been used to treat dye-containing effluents, such as, coagulation/flocculation (Verma et al., 2012), biosorption (Srinivasan and Viraraghavan, 2010), adsorption (Moussavi and Khosravi, 2011), bacterial decolorization (Saratale et al., 2011), advanced oxidation (Koprivanac and Kusic, 2008) and others (Koprivanac and Kusic, 2008; Gupta and Ali, 2013). It is recognized in literature that the adsorption onto chitosan is an emerging alternative technology to remove dyes from aqueous media (Crini and Badot, 2008; Wan Ngah et al., 2011).

Chitosan can be obtained from natural resources and its use as adsorbent is extremely cost effective. In addition, the adsorption capacities and adsorption rates are high (Crini and Badot, 2008). Studies have focused on chemical and physical modifications to improve the performance of chitosan as dye adsorbent (Kyzas and Lazaridis, 2009; Wan Ngah et al., 2011; Li et al., 2012; Mirmohseni et al., 2012; Zhu et al., 2012; Dotto

* Corresponding author.
E-mail addresses: guilherme_dotto@yahoo.com.br (G.L. Dotto), celene.buriol@gmail.com (C. Buriol), dqmpinto@furg.br (L.A.A. Pinto).
Received 22 August 2013; Received in revised form 28 January 2014; Accepted 17 March 2014
http://dx.doi.org/10.1016/j.cherd.2014.03.013

Nomenclature

a_{RP}	Redlich–Peterson constant, $(L\,mg^{-1})^{\beta}$
Bi_s	Biot number, dimensionless
$C(t)$	dye concentration in bulk solution, $mg\,L^{-1}$
$C(x,t)$	dye concentration within the chitosan film varying with x and t, $mg\,L^{-1}$
C_0	initial dye concentration in bulk solution, $mg\,L^{-1}$.
C_e	dye concentration in bulk solution at equilibrium, $mg\,L^{-1}$
$C_s(t)$	dye concentration at $x = L/2$, $mg\,L^{-1}$
D_{AB}	molecular diffusion coefficient, $m^2\,s^{-1}$
D_p	effective pore volume diffusion coefficient, $m^2\,s^{-1}$
D_s	surface diffusion coefficient, $m^2\,s^{-1}$
k_f	external mass transfer coefficient, $m\,s^{-1}$
k_{RP}	Redlich–Peterson constant, $L\,g^{-1}$
L	thickness of chitosan film, m or μm
m	mass of chitosan film, g
M_B	molecular weight of water, $g\,mol^{-1}$
N	number of experimental points
$q(t)$	mass of dye adsorbed per gram of adsorbent, $mg\,g^{-1}$
$q(x,t)$	mass of dye adsorbed varying with x and t, $mg\,g^{-1}$
q_e	mass of dye adsorbed at equilibrium, $mg\,g^{-1}$
q_0	mass of dye adsorbed at equilibrium with a hypothetical liquid concentration, $mg\,g^{-1}$
S	external surface area per mass of adsorbent, $cm^2\,g^{-1}$
t	time, min or s
T	temperature, K
V	volume of solution, L or m^3
V_A	molar volume of solute at its normal boiling temperature, $cm^3\,mol^{-1}$
x	spatial direction, m

Greek symbols

β	Redlich–Peterson constant, dimensionless
ε_p	void fraction of the chitosan film, dimensionless
η_B	viscosity of water, cp
γ	defined in Eq. (14.1)
λ_n	defined in Eq. (13.2)
ρ_p	apparent density of the chitosan film, $g\,L^{-1}$
ρ_s	solid density of the chitosan film, $g\,L^{-1}$
τ	tortuosity factor, dimensionless
φ	association parameter of water, dimensionless
$\psi(t)$	defined in Eq. (13.1)

et al., 2013). In this way, some chitosan based materials were developed, for example, foam (Li et al., 2012), hollow fibers (Mirmohseni et al., 2012), hydrogels (Zhu et al., 2012) and films (Dotto et al., 2013). Recently, Dotto et al. (2013) applied chitosan films to remove food dyes from aqueous solutions. Their study was focused on the equilibrium isotherms, thermodynamic and interaction analysis. However, the design of an adsorption system to treat colored effluents also requires the investigation of the adsorption kinetics (Crini and Badot, 2008). Generally, in the studies about dye removal on chitosan based materials, the kinetic investigation is based on the adsorption reaction models (Kyzas and Lazaridis, 2009; Dotto and Pinto, 2011a; Wan Ngah et al., 2011; Li et al., 2012; Mirmohseni et al., 2012; Zhu et al., 2012; Dotto et al., 2013).

The adsorption reaction models (pseudo-first order and pseudo-second order) assumes that the adsorption kinetics is exclusively controlled by the adsorption rate of the solute on the surface of the adsorbent, and the intraparticle diffusion and external mass transfer can be ignored (Ocampo-Pérez et al., 2012). Furthermore, is considered that the adsorption kinetics can be represented in the same manner as the rate of a chemical reaction (Qiu et al., 2009). Based on these models, it is not possible to obtain the mass transfer parameters and identify the rate controlling step. On the other hand, the diffusional mass transfer models are constructed on the basis of three consecutive steps: external mass transfer, intraparticle diffusion (pore volume diffusion, surface diffusion, or a combination of both mechanisms) and adsorption on an active site; and so represents more realistically the adsorption kinetics (Qiu et al., 2009; Ocampo-Perez et al., 2010, 2011; Dotto and Pinto, 2011b, 2012; Ocampo-Pérez et al., 2012). Since there are few reports in the literature about the application of diffusional mass transfer models in the adsorption of food dyes on chitosan films, detailed studies are necessary in this field.

This work aimed to develop a diffusional mass transfer model to represent the adsorption kinetics of erythrosine B and indigo carmine on chitosan films. Chitosan films were prepared and characterized by scanning electron microscopy (SEM), X-ray mapping and mechanical properties. The model was developed considering the external mass transfer and intraparticle diffusion steps, and was employed to study the experimental curves under different conditions of stirring rate and initial dye concentration. Furthermore, the mass transfer parameters were estimated and interpreted in detail.

2. Materials and methods

2.1. Dyes

The dyes used in this work were: erythrosine B (acid red 51; xanthene dye; molecular weight 879.86 $g\,mol^{-1}$; C.I. 45,430; $\lambda_{max} = 526$ nm; molecular size 11.0 Å) and indigo carmine (FD&C blue no. 2; indigoid dye; molecular weight 466.34 $g\,mol^{-1}$; C.I. 73,015; $\lambda_{max} = 610$ nm; molecular size 16.8 Å). These dyes (purity higher than 85%) were supplied by a local manufacturer (Duas Rodas Ind.) and were used without further purification. The chemical structures of the dyes are shown in Fig. 1. Distilled water was used to prepare all solutions. All reagents were of analytical-grade.

2.2. Preparation of chitosan films

Firstly, chitosan in powder form (deacetylation degree of 85 ± 1%, viscosity average molecular weight of 150 ± 3 kDa and particle size of 72 ± 3 μm) was obtained from shrimp wastes (*Penaeus brasiliensis*) by the following steps: demineralization, deproteinization, deodorization, deacetylation, purification and drying (Weska et al., 2007; Dotto et al., 2011a). After, chitosan films were obtained by casting technique as follows: chitosan powder was dissolved in acetic acid solution using moderate magnetic stirring (Marte, MAG-01H, Brazil) at room temperature. This solution was centrifuged (Fanem, 206 BL, Brazil) and poured onto a level plexiglas plate. Then, chitosan films were obtained by solvent evaporation and conditioned in desiccators prior to the use (Dotto et al., 2011b, 2013). More

Please cite this article in press as: Dotto, G.L., et al., Diffusional mass transfer model for the adsorption of food dyes on chitosan films. Chem. Eng. Res. Des. (2014), http://dx.doi.org/10.1016/j.cherd.2014.03.013

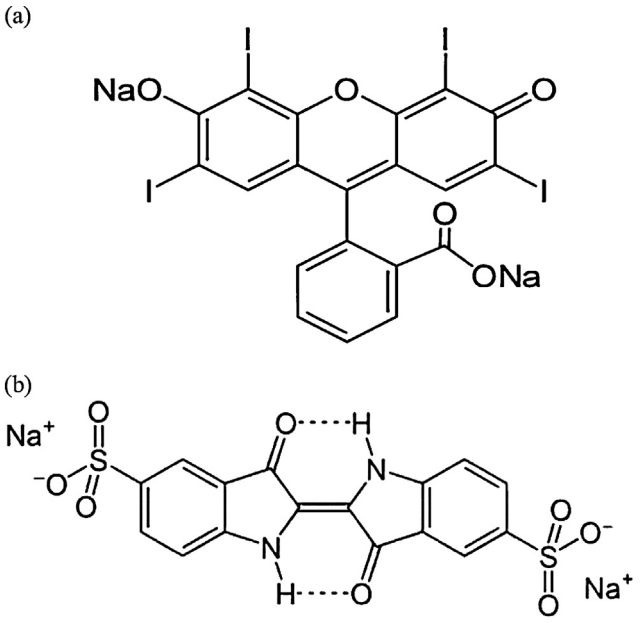

Fig. 1 – Chemical structures of the dyes: (a) erythrosine B and (b) indigo carmine.

detailed procedures can be obtained in our previous works (Weska et al., 2007; Dotto et al., 2011a,b, 2013).

2.3. *Characterization of chitosan films*

The textural characteristics of the chitosan films were observed before and after the adsorption process by scanning electron microscopy (SEM) (Jeol, JSM-6610LV, Japan) (Goldstein et al., 1992). X-ray mappings of iodine (erythrosine B) and sulfur (indigo carmine) were carried out in the chitosan films after the adsorption process (Jeol, JSM-6610LV, Japan) (Goldstein et al., 1992). The tensile strength and elongation were measured by a texture analyzer (Stable Micro Systems, TA-XT-2i, UK) according to the procedures of the American society for testing and materials (ASTM, 2001). The dimensions (length, width and thickness) were obtained by a digital micrometer (Insize, IP54, Brazil) with 0.0010 mm of resolution. The external surface area per mass of adsorbent (S) was calculated from the dimensions, based on the spatial geometry of the chitosan films. The solid density (ρ_s) was obtained from the literature (Piccin et al., 2011), the apparent density (ρ_p) was determined by the mass/volume relation in an analytical balance (Marte, AY220, Brazil), and the void fraction (ε_p) of the chitosan films was estimated by Eq. (1) (Dotto and Pinto, 2012):

$$\varepsilon_p = 1 - \frac{\rho_p}{\rho_s} \tag{1}$$

2.4. *Procedure to obtain the experimental kinetic curves*

In order to obtain the experimental kinetic curves, batch adsorption assays were carried out in a jar-test (Nova etica, 218 MBD, Brazil), at different conditions of stirring rate (80 and 200 rpm) and initial dye concentration (20, 60 and100 mg L^{-1}). The other experimental conditions were based on preliminary tests and literature (Hessel et al., 2007; Crini and Badot, 2008). Dye stock solutions (1.00 g L^{-1}) were prepared (pH was adjusted to 7.0), and all subsequent tests were realized by diluting these solutions. 500 mg of chitosan films (divided in portions of 1 cm × 1 cm (this size was selected in order to facilitate the phase separation after the adsorption process)) were added in 1.0 L of solutions with desired initial dye concentration (20, 60 or 100 mg L^{-1}) and these solutions were agitated (80 or 200 rpm) at room temperature (298 ± 2 K). Samples were collected in preset time intervals (2, 4, 6, 8, 10, 15, 20, 25, 30, 40, 50, 60, 80, 100 and 120 min) and also at equilibrium (the equilibrium was considered attained when the dye concentration in the liquid phase did not present difference between three consecutive measures). The dyes concentration was determined by spectrophotometry (Biospectro, SP-22, Brazil) at 526 nm and 610 nm for erythrosine B and indigo carmine, respectively. Blanks were performed and experiments were carried out in replicate. The mass of dye adsorbed per gram of adsorbent at any time ($q(t)$), and the mass of dye adsorbed at equilibrium (q_e) were calculated by Eqs. (2) and (3), respectively:

$$q(t) = \frac{(C_0 - C(t))}{m} V \tag{2}$$

$$q_e = \frac{(C_0 - C_e)}{m} V \tag{3}$$

3. Model

3.1. *Model development*

Generally, in solid–liquid adsorption systems it is accepted that the mass transfer can occur in three steps: external mass transfer, intraparticle diffusion and adsorption on active sites. The intraparticle diffusion may be controlled by pore volume diffusion, surface diffusion or a combination of both mechanisms (Ruthven, 1984; Qiu et al., 2009; Ocampo-Perez et al., 2010; Dotto and Pinto, 2011b; Ocampo-Perez et al., 2011; Wegmann et al., 2011; Baz-Rodríguez et al., 2012; Dotto and Pinto, 2012; Ocampo-Pérez et al., 2012). In this work, the dyes adsorption on active sites was considered instantaneous (Crini and Badot, 2008; Dotto et al., 2013), and thus, no affects the adsorption rate. Furthermore, the following preliminary assumptions were made for the considered system: the adsorption occurs at 298 K; the pores of the chitosan films are saturated with liquid; the mass transport by convection within the pores is negligible; the intraparticle diffusion can occur by pore volume diffusion, surface diffusion or both; the values of effective pore volume diffusion coefficient (D_p) and surface diffusion coefficient (D_s) are constant. Based on the above assumptions, the distribution of C and q into the chitosan film can be represented by the general diffusive model (Suzuki, 1990; Do, 1997), as demonstrated in Eq. (4):

$$\varepsilon_p \frac{\partial C}{\partial t} + \rho_s(1-\varepsilon_p)\frac{\partial q}{\partial t} = D_p \nabla^2 C + \rho_s(1-\varepsilon_p) D_s \nabla^2 q \tag{4}$$

In Eq. (4), the first term of the left is the dye accumulation in the pore volume of chitosan films and the second term is the accumulation due to the dye adsorption on the surface of chitosan films. The first and second terms of the right are relative to the pore volume diffusion and surface diffusion, respectively.

As observed in Table 1 (Section 4.1), the length and width of the chitosan films are very higher than the thickness, so, the mass transfer can be considered in the x direction, consequently, for Cartesian coordinates, Eq. (4) can be simplified in

Table 1 – Chitosan films characteristics.

	Characteristic	Value
Mechanical properties[a]	Tensile strength (MPa)	27.9 ± 2.5
	Elongation (%)	12.5 ± 1.0
Dimensions[a]	Length (cm)	1.00 ± 0.01
	Width (cm)	1.00 ± 0.01
	Thickness (μm)	75 ± 1
Density, void fraction and external surface area	ρ_s (g L^{-1})	1550
	ρ_p (g L^{-1})	1333
	ε_p	0.140
	S (cm^2 g^{-1})	200

[a] Mean ± standard error (n = 3).

the form of Eq. (5):

$$\varepsilon_p \frac{\partial C(x,t)}{\partial t} + \rho_s(1-\varepsilon_p)\frac{\partial q(x,t)}{\partial t} = D_p \frac{\partial^2 C(x,t)}{\partial x^2} + \rho_s(1-\varepsilon_p)D_s \frac{\partial^2 q(x,t)}{\partial x^2} \quad (5)$$

Low values of void fraction (ε_p) were observed for the chitosan films (Table 1), so, it can be assumed that the surface diffusion is the predominant intraparticle mass transfer mechanism. In this way the terms which contains $C(x,t)$ (Eq. (5)) can be neglected, leading to Eq. (6):

$$\rho_s(1-\varepsilon_p)\frac{\partial q(x,t)}{\partial t} = \rho_s(1-\varepsilon_p)D_s \frac{\partial^2 q(x,t)}{\partial x^2} \quad (6)$$

Eq. (6) can be simplified in the form of Eq. (7):

$$\frac{\partial q(x,t)}{\partial t} = D_s \frac{\partial^2 q(x,t)}{\partial x^2} \quad (7)$$

In this way, it is assumed that in the adsorption of food dyes, the accumulation rate within the chitosan film is due to the surface diffusion in the x direction. Leading into account the external mass transfer from the bulk solution to the chitosan film surface, the initial and boundary conditions are presented in Eqs. (8)–(10). The representative illustration of the problem considered in this work is shown in Fig. 2.

$$t = 0, \quad 0 \le x \le \frac{L}{2} \Rightarrow q(x,t) = 0 \quad (8)$$

$$\left.\frac{\partial q(x,t)}{\partial x}\right|_{x=0} = 0 \quad (9)$$

$$\rho_s(1-\varepsilon_p)D_s \left.\frac{\partial q(x,t)}{\partial x}\right|_{x=L/2} = k_f(C(t) - C_s(t)) \quad (10)$$

For the dyes adsorption onto chitosan films, at $x = L/2$, the equilibrium relation is given by the Redlich–Peterson isotherm (Dotto et al., 2013), as presented in Eq. (11):

$$q(x = L/2, t) = \frac{k_{RP}C_s(t)}{1 + (a_{RP}C_s(t)^{\beta})} \quad (11)$$

The estimated values of a_{RP}, k_{RP} and β were, respectively, 2.01 (L mg^{-1})$^{\beta}$, 396.0 L g^{-1} and 0.99 for erythrosine B and 4.75 (L mg^{-1})$^{\beta}$, 411.1 L g^{-1} and 0.80 for indigo carmine (Dotto et al., 2013). In addition to Eqs. (7)–(11), Eqs. (2) and (12) were used to solve the model (Suzuki, 1990; Baz-Rodríguez et al., 2012).

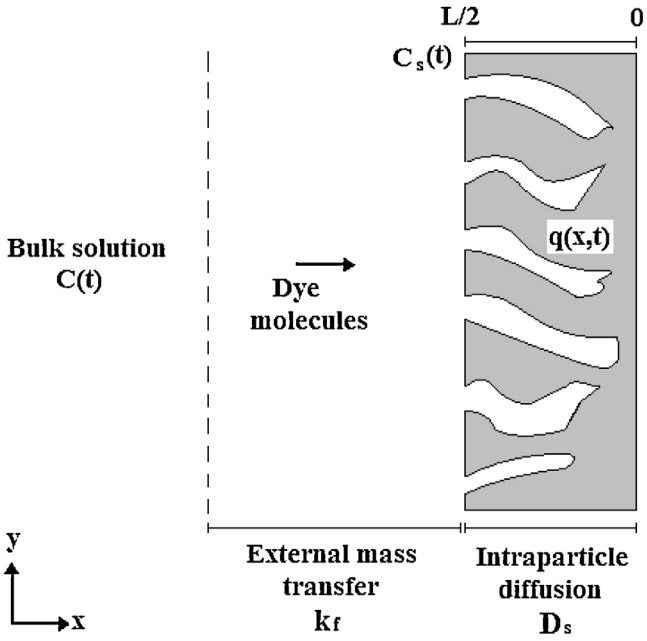

Fig. 2 – Transport of the dye molecules from the solution to the chitosan film (illustrative representation).

$$q(t) = \frac{2}{L}\int_0^{L/2} q(x,t)\,dx \quad (12)$$

3.2. Model solution

The mathematical model is the simultaneous solution of Eqs. (2) and (7)–(12). Using the separation of variables method, it can be proved that Eq. (13) is the unique solution of Eq. (7) with the above initial and boundary conditions (Section 3.1) (Strauss, 2008).

$$q(x,t) = \psi(t) + \frac{4}{\pi}\sum_{n=0}^{+\infty}\frac{(-1)^{n+1}}{1+2n}e^{D_s\lambda_n^2 t}\left(\int_0^t e^{D_s\lambda_n^2\tau}\psi'(\tau)d\tau\right) \times \cos\left((1+2n)\frac{\pi x}{L}\right) \quad (13)$$

being

$$\psi(t) = \frac{k_{RP}C_s(t)}{1 + (a_{RP}C_s(t)^{\beta})} \quad (13.1)$$

$$\lambda_n = (1+2n)\frac{\pi}{L} \quad (13.2)$$

By Eqs. (2), (10) and (13), it can be obtained that $C(t)$, $C_s(t)$ and $q(t)$ satisfies Eqs. (14) and (15) (Strauss, 2008):

$$C(t) = e^{(-m\gamma t/V)}\left(\int_0^t \frac{m\gamma}{V}C_s(\tau)e^{(m\gamma\tau/V)}d\tau + C_0\right) \quad (14)$$

where

$$\gamma = \frac{2k_f}{L\rho_s(1-\varepsilon_p)} \quad (14.1)$$

$$q(t) = \psi(t) - \frac{8}{\pi^2}\sum_{n=0}^{+\infty}\frac{e^{-D_s\lambda_n^2 t}}{(1+2n)^2}\left(\int_0^t e^{D_s\lambda_n^2\tau}\psi'(\tau)d\tau\right) \quad (15)$$

3.3. Estimation of the mass transfer parameters

To obtain the surface diffusion coefficient (D_s), the integrals (in Eqs. (14) and (15)) were approximated by the numerical quadrature's method (Burden and Faires, 2011), being considered the first two terms of the series in Eq. (15). Then, a system with Eqs. (2), (14) and (15) was matched with the experimental data, and the more adequate value for D_s was estimated by minimizing the sum of the least squares (*SSR*) (Eq. (16)) (Ocampo-Pérez et al., 2012):

$$SSR = \sum_1^N (q(t)_{experimental} - q(t)_{predicted})^2 \quad (16)$$

The external mass transfer coefficient (k_f) was estimated by the procedure proposed by Furusawa and Smith (1973) as demonstrated in Eq. (17):

$$V\frac{dC(t)}{dt} = -mSk_f(C(t) - C_s(t)) \quad (17)$$

When $t \to 0$ then $C_s(t) \to 0$ and $C(t) \to C_0$. Substituting these conditions in Eq. (17), Eq. (18) is obtained:

$$\left[\frac{d(C(t)/C_0)}{dt}\right] = \frac{-mSk_f}{V} \quad (18)$$

The term in the right of Eq. (18) is the slope of the curve $C(t)/C_0$ versus t, at $t=0$ and was estimated by using the first three data points.

3.4. Model fit evaluation

The quality of the fit between the experimental data ($q(t)_{experimental}$) and the predicted data ($q(t)_{predicted}$) was evaluated by the average relative error (*ARE*), as presented in Eq. (19) (Ocampo-Perez et al., 2011):

$$ARE = \frac{100}{N}\sum_1^N \left|\frac{q(t)_{experimental} - q(t)_{predicted}}{q(t)_{experimental}}\right| \quad (19)$$

4. Results and discussion

4.1. Chitosan films characteristics

The SEM images of chitosan films before adsorption process (a), adsorbed with erythrosine B (b) and adsorbed with indigo carmine (c) are shown in Fig. 3. It can be seen in Fig. 3(a) that the chitosan films presented a homogeneous surface with some cavities and protuberances. Some porous were also observed. After the adsorption process (Fig. 3(b) and (c)), the external surface of the chitosan films was smoothed and fewer pores were observed. This suggests that the dyes were adhered on the chitosan films. Fig. 4 shows the X-ray mappings of iodine (erythrosine B) and sulfur (indigo carmine) in the chitosan films after the adsorption process, at $x = L/2$ and $x = 0$. The presence of iodine and sulfur at $x = L/2$ (Fig. 4(a) and (c), respectively) confirms that the external surface of the chitosan films was covered by the dyes. Furthermore, the presence of

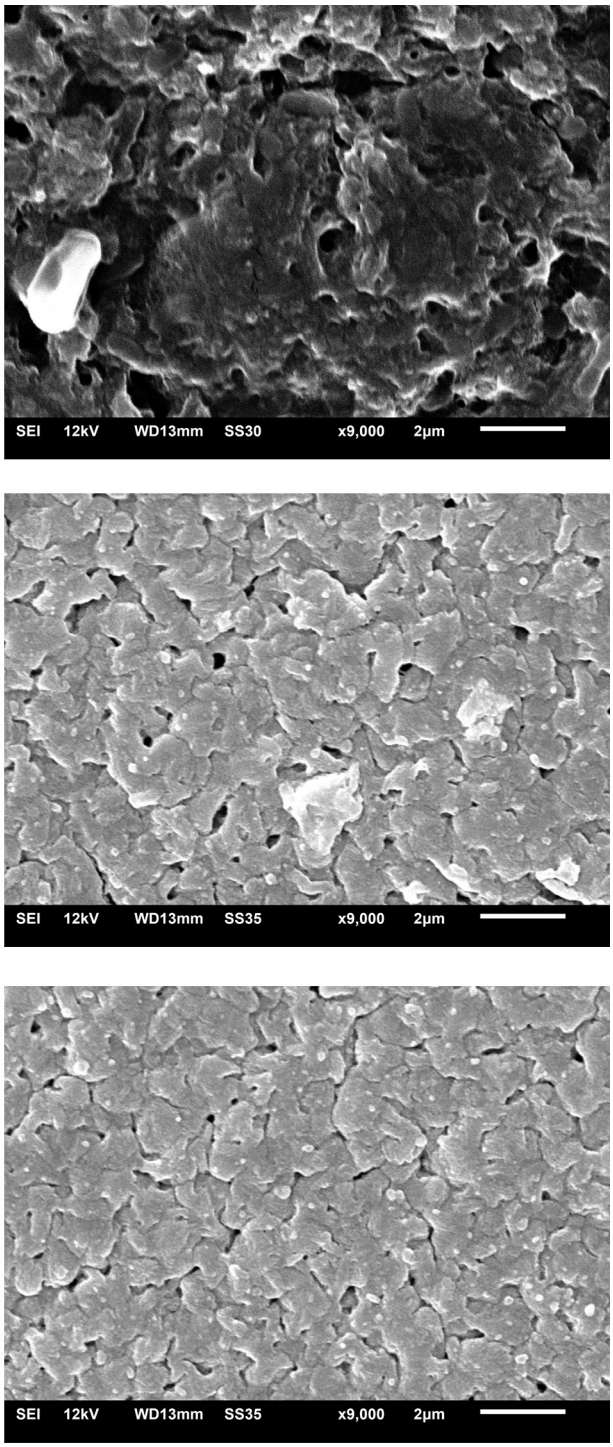

Fig. 3 – SEM images of chitosan films: (a) before adsorption process, (b) adsorbed with erythrosine B and (c) adsorbed with indigo carmine.

iodine and sulfur at $x = 0$ (Fig. 4(b) and (d), respectively) indicated that the dyes were transferred within the chitosan films.

The chitosan film dimensions (Table 1) confirms the assumption that the mass transfer is mainly in x direction. The low values of void fraction (ε_p) (Table 1) suggest that the mass transfer occurs mainly in the surface of chitosan films. This fact help to support that the surface diffusion is the predominant intraparticle mass transfer mechanism in the adsorption of food dyes onto chitosan films. In relation to the mechanical properties (Table 1), it is possible to affirm that the chitosan films showed good values for tensile strength and elongation

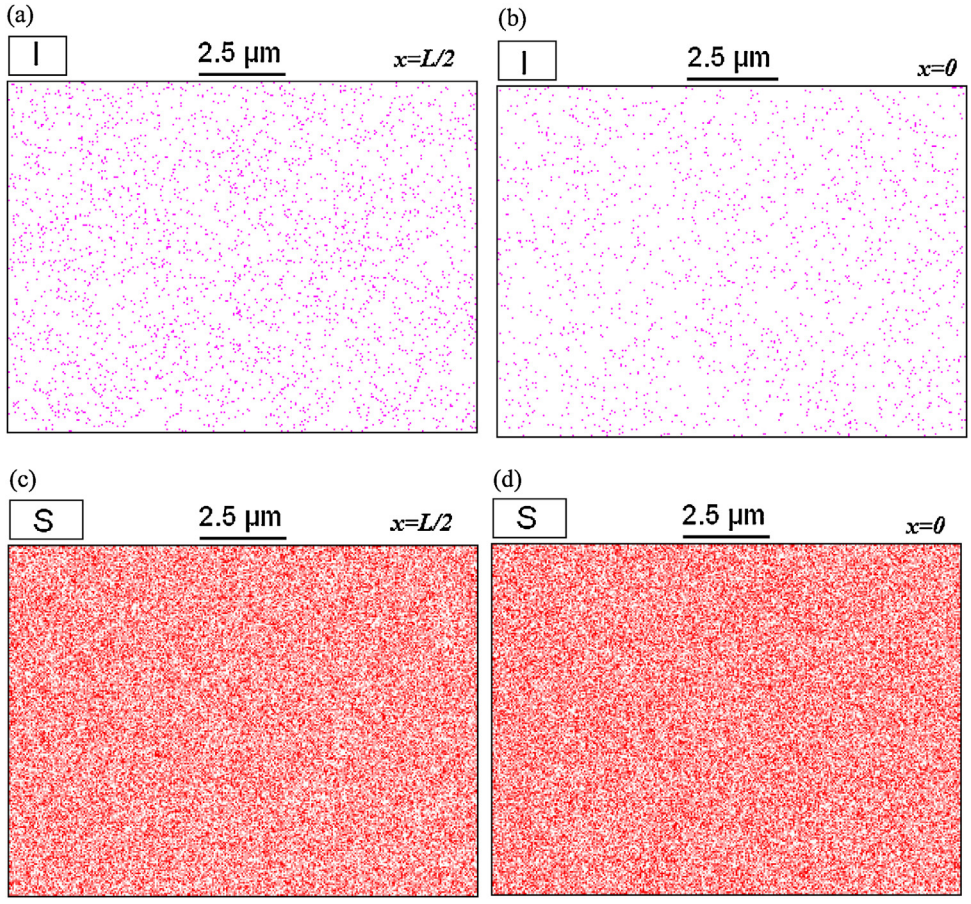

Fig. 4 – X-ray mappings of iodine (erythrosine B) and sulfur (indigo carmine) in the chitosan films after the adsorption process: (a) iodine at $x = L/2$, (b) iodine at $x = 0$, (c) sulfur at $x = L/2$ and (d) sulfur at $x = 0$.

(Fajardo et al., 2012). These properties facilitate the phase separation after adsorption (Dotto et al., 2013).

4.2. *Model validation and interpretation of the experimental curves*

The experimental adsorption kinetic curves of erythrosine B and indigo carmine on chitosan films were obtained under different conditions of stirring rate (80–200 rpm) and initial dye concentration (20–100 mg L^{-1}). These curves were modeled by a diffusional mass transfer model considering the external mass transfer and intraparticle diffusion steps. Based on the experimental system and previously studies, it was also assumed that the mass transfer occurred only in x direction and the intraparticle diffusion step is mainly due to surface diffusion. Furthermore, the equilibrium relation was the Redlich–Peterson isotherm. For all kinetic curves, the values of average relative error (ARE) ranged from 1.51 to 3.59%, demonstrating that the proposed diffusional mass transfer model agreed very well with the experimental data. This is an indicative that the surface diffusion was the rate limiting step. The good concordance between the experimental and modeled data can be visualized in Figs. 5 (erythrosine B) and 6 (indigo carmine).

The stirring rate effect on the experimental kinetic curves is presented in Figs. 5(a) (erythrosine B) and 6(a) (indigo carmine). It can be seen in these figures, that, for both dyes, the stirring rate increase from 80 to 200 rpm caused an increase in the $q(t)$ values (the model also followed this tendency). This can be occurred because, the stirring rate increase leads to an increase in the energy dissipation and turbulence in the mixing zone, consequently, the boundary layer thickness is decreased, facilitating the external mass transfer (Ruthven, 1984; Suzuki, 1990). Dotto and Pinto (2012) analyzed the mass transfer kinetics in the biosorption of synthetic dyes onto *Spirulina platensis* nanoparticles. They verified similar trend, when the stirring rate was increased from 50 to 225 rpm. Ocampo-Perez et al. (2010), studying the adsorption of pyridine onto granular activated carbon, found that the external mass transfer was affected by the stirring rate increase from 100 to 200 rpm.

Fig. 5(b) (erythrosine B) and 6(b) (indigo carmine) show the initial dye concentration effect on the kinetic curves. It was found that, for both dyes, the initial dye concentration (C_0) increase from 20 to 100 mg L^{-1} caused an increase in the $q(t)$ values (the model also followed this tendency). This behavior can be explained by two facts: (1) at higher values of C_0, the concentration gradient between the bulk solution and the adsorbent external surface is higher, facilitating the external mass transfer (this can be verified mathematically by the combination of Eqs. (2), (17) and (18)); (2) at higher values of C_0, the driving force $C(t)$–$C_s(t)$ is higher, consequently, the mass flux of dye by surface diffusion is increased, as mathematically demonstrated in Eq. (10). Similar behavior was obtained by Choy et al. (2004) in the adsorption of acid dyes from aqueous solutions onto activated carbon.

In brief, it was found that, under the considered conditions of stirring rate and initial dye concentration, the diffusional mass transfer model used in this work is adequate to represent the adsorption kinetics of erythrosine B and indigo carmine on

Please cite this article in press as: Dotto, G.L., et al., Diffusional mass transfer model for the adsorption of food dyes on chitosan films. Chem. Eng. Res. Des. (2014), http://dx.doi.org/10.1016/j.cherd.2014.03.013

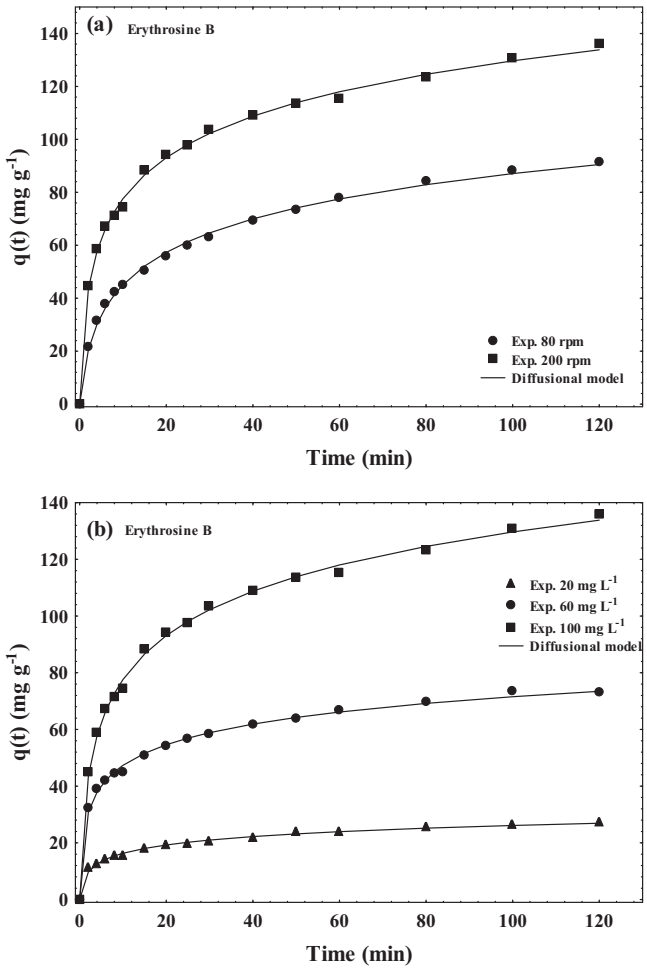

Fig. 5 – Experimental kinetic curves for the adsorption of erythrosine B on chitosan films: (a) stirring rate effect and (b) initial concentration effect.

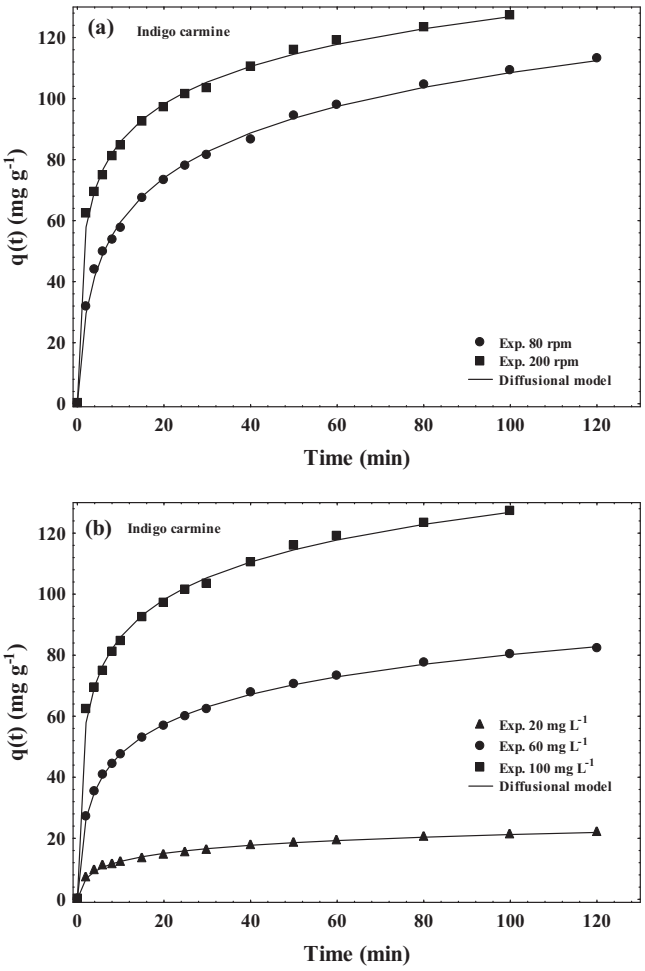

Fig. 6 – Experimental kinetic curves for the adsorption of indigo carmine on chitosan films: (a) stirring rate effect and (b) initial concentration effect.

chitosan films. This implies that the external mass transfer and intraparticle diffusion steps should be considered, being that the surface diffusion is the predominant intraparticle mass transfer mechanism.

4.3. *Interpretation of the mass transfer parameters*

Table 2 shows the mass transfer parameters for the adsorption of erythrosine B and indigo carmine under different experimental conditions. In order to prove that the surface diffusion is the predominant intraparticle mass transfer mechanism (as mentioned in Section 4.2), the values of D_{AB} and D_p were calculated and compared with D_s (Table 2). The values of D_{AB} and D_p were calculated by Eqs. (20) and (21), respectively (Wilke and Chang, 1955; Valderrama et al., 2008):

$$D_{AB} = 7.4 \times 10^{-8} \left[\frac{(\varphi M_B)^{0.5} T}{\eta_B V_A^{0.6}} \right] \quad (20)$$

$$D_p = \frac{D_{AB} \varepsilon_p}{\tau} \quad (21)$$

being

$$\tau = \frac{(2 - \varepsilon_p)^2}{\varepsilon_p} \quad (22)$$

The values of D_p were $2.20 \times 10^{-12}\ m^2\ s^{-1}$ for erythrosine B and $2.69 \times 10^{-12}\ m^2\ s^{-1}$ for indigo carmine. Since $D_p \ggg D_s$ (Table 2), the transference of the dyes by pore volume diffusion can be neglected (confirming the assumption in Section 3.1), and it can be concluded that the surface diffusion was the rate limiting step. Similar behavior was found by Ocampo-Perez et al. (2010), studying the adsorption of pyridine onto granular activated carbon. They found that the surface diffusion represented more than 93.5% of total intraparticle diffusion, confirming that surface diffusion was the mechanism controlling the overall adsorption rate.

Table 2 shows three aspects regarding to the external mass transfer coefficient (k_f): (1) it was found that the stirring rate increase caused an increase in the k_f values. This occurred due to the increase in the system mobility (as explained in Section 4.2), and implies that the transference of the dyes across the external layer was facilitated at 200 rpm; (2) the initial dye concentration increase caused an increase in the k_f values. This shows that at higher initial dye concentrations, the external mass transfer resistance was decreased. Similar dependences of k_f in relation to the stirring rate and initial concentration were found in the phenol adsorption onto organobentonite (Ocampo-Perez et al., 2011); (3) In general, the k_f values for indigo carmine were lower than the k_f values for erythrosine B. This can occurred, because the indigo carmine dye has a higher and more ramified molecular structure (Fig. 1), hindering its transference across the external layer. Similar behavior

Please cite this article in press as: Dotto, G.L., et al., Diffusional mass transfer model for the adsorption of food dyes on chitosan films. Chem. Eng. Res. Des. (2014), http://dx.doi.org/10.1016/j.cherd.2014.03.013

Table 2 – Mass transfer parameters for the adsorption of erythrosine B and indigo carmine under different experimental conditions.

Dye	Stirring rate (rpm)	C_0 (mg L^{-1})	C_e (mg L^{-1})	q_e (mg g^{-1})	$k_f \times 10^4$ (m s^{-1})	$D_s \times 10^{14}$ (m^2 s^{-1})	Bi_s
Erythrosine B	80	20	0.1	39.7	1.39	0.41	478.5
		60	0.6	118.8	1.52	6.69	32.2
		100	2.7	194.6	1.74	11.10	22.7
	200	20	0.1	39.7	1.95	1.06	260.3
		60	0.6	118.8	2.02	9.06	31.7
		100	2.7	194.6	2.17	16.40	19.1
Indigo carmine	80	20	0.2	39.5	1.32	1.91	98.7
		60	6.4	107.2	1.45	11.61	19.7
		100	22.6	154.8	1.76	13.70	23.3
	200	20	0.2	39.5	1.41	1.80	111.3
		60	6.4	107.2	1.90	12.10	24.7
		100	22.6	154.8	2.15	22.90	17.0

was verified in the biosorption of acid blue 9 and FD&C red 40 on *S. platensis* nanoparticles (Dotto and Pinto, 2012).

In relation to the D_s values (Table 2), it was verified that the higher values were obtained at higher initial dye concentrations. Furthermore, higher D_s values were obtained for the indigo carmine dye. The first fact can be explained as follows: as expected, the initial dye concentration (C_0) increase caused an increase in the q_e values (Table 2) and, so, the D_s values increased (Ruthven, 1984; Suzuki, 1990; Do, 1997). This can occurred because, at first, the dye molecules are adsorbed on the high energy sites (or more available), and so, few of the adsorbed molecules had enough energy to move along the surface from one site to another. Since the high energy sites have been occupied, the dye molecules would be adsorbed on the low-energy sites. Therefore, a greater number of molecules had enough energy to move from one site to the other (Suzuki, 1990; Ocampo-Perez et al., 2011). The second fact can be explained as follows: the indigo carmine dye has sulfonated groups in its structure, and these groups have high affinity with the protonated amino groups on the chitosan films internal surface (Crini and Badot, 2008). In this way the transport of this dye is facilitated on the surface, providing high D_s values. The D_s values obtained in this work were in the range of 10^{-14} m^2 s^{-1} (Table 2). Lee and McKay (2004) obtained D_s values of 3.0×10^{-14} m^2 s^{-1} for the adsorption of basic yellow 21 on activated carbon, and 12.0×10^{-14} m^2 s^{-1} for the adsorption of basic blue 69 on silica.

In order to verify the predominance of surface diffusion in relation to the external mass transfer, the surface diffusion modified Biot number, (Bi_s) was used. The surface diffusion modified Biot number is given by Eq. (23) (Weber and Di Giano, 1995):

$$Bi_s = \frac{k_f L C_0}{2\rho_s D_s q_0} \quad (23)$$

In this work, the surface diffusion modified Biot number ranged from 17.0 to 478.5 (Table 2). According to the literature, for $Bi_s < 0.5$, it exists a complete dominance of the external mass transfer, while for $Bi_s > 10$ a considerable dominance of the surface diffusion exists (Costa and Rodrigues, 1985; Li et al., 2003). In this way, the Bi_s values obtained in this work corroborate that, in the adsorption of erythrosine B and indigo carmine on chitosan films, the surface diffusion is the rate limiting step.

5. Conclusion

In this work, a diffusional mass transfer model was used to represent the adsorption of erythrosine B and indigo carmine on chitosan films under different conditions of stirring rate and initial dye concentration. The diffusional mass transfer model agreed very well with the experimental curves, indicating that the surface diffusion was the predominant intraparticle mass transfer mechanism. The external mass transfer coefficient (k_f) ranged from 1.32×10^{-4} to 2.17×10^{-4} m s^{-1}. The values of surface diffusion coefficient (D_s) were in the range from 0.41×10^{-14} to 22.90×10^{-14} m^2 s^{-1}. Since $D_p \ggg D_s$ and $17.0 \leq Bi_s \geq 478.5$, it was proved that in the adsorption of erythrosine B and indigo carmine on chitosan films, the surface diffusion was the rate limiting step.

Acknowledgements

The authors would like to thank CAPES (Brazilian Agency for Improvement of Graduate Personnel) and CNPq Rede Nanobiotec-Brazil/Edital 4CII2008 (National Council of Science and Technological Development) for the financial support. Furthermore, the authors would like to thank CEME-SUL/FURG (Electron Microscopy Center of southern/Federal University of Rio Grande) due to the scanning electron microscopy images and X-ray mappings.

References

American Society for Testing and Materials (ASTM), 2001. Standard test Methods for Tensile Properties of Thin Plastic Sheeting (Standard D882-02, 162–170), Philadelphia.

Baz-Rodríguez, S.A., Ocampo-Pérez, R., Ruelas-Leyva, J.P., Aguilar-Madera, C.G., 2012. Effective transport properties for the pyridine-granular activated carbon adsorption system. Braz. J. Chem. Eng. 29, 599–611.

Burden, R.L., Faires, J.D., 2011. Numerical Analysis. Cengage Learning, Boston.

Choy, K.K.H., Porter, J.F., McKay, G., 2004. Film-pore diffusion models: analytical and numerical solutions. Chem. Eng. Sci. 59, 501–512.

Costa, C., Rodrigues, A.E., 1985. Intraparticle diffusion of phenol in macroreticular adsorbents: modeling and experimental study of batch and CSTR adsorbers. Chem. Eng. Sci. 40, 983–993.

Crini, G., Badot, P.M., 2008. Application of chitosan, a natural aminopolysaccharide, for dye removal from aqueous solutions by adsorption processes using batch studies: a review of recent literature. Prog. Polym. Sci. 33, 399–447.

Do, D.D., 1997. Dynamics of adsorption in heterogeneous solids. Stud. Surf. Sci. Catal. 104, 777–835.
Dotto, G.L., Moura, J.M., Cadaval Jr., T.R.S., Pinto, L.A.A., 2013. Application of chitosan films for the removal of food dyes from aqueous solutions by adsorption. Chem. Eng. J. 214, 8–16.
Dotto, G.L., Pinto, L.A.A., 2011a. Adsorption of food dyes onto chitosan: optimization process and kinetic. Carbohydr. Polym. 84, 231–238.
Dotto, G.L., Pinto, L.A.A., 2011b. Adsorption of food dyes acid blue 9 and food yellow 3 onto chitosan: stirring rate effect in kinetics and mechanism. J. Hazard. Mater. 187, 164–170.
Dotto, G.L., Pinto, L.A.A., 2012. Analysis of mass transfer kinetics in the biosorption of synthetic dyes onto *Spirulina platensis* nanoparticles. Biochem. Eng. J. 68, 85–90.
Dotto, G.L., Souza, V.C., Moura, J.M., Moura, C.M., Pinto, L.A.A., 2011b. Influence of drying techniques on the characteristics of chitosan and the quality of biopolymer films. Drying Technol. 29, 1784–1791.
Dotto, G.L., Souza, V.C., Pinto, L.A.A., 2011a. Drying of chitosan in a spouted bed: the influences of temperature and equipment geometry in powder quality. LWT Food Sci. Technol. 44, 1786–1792.
Downham, A., Collins, P., 2000. Colouring our food in the last and next millennium. Int. J. Food Sci. Technol. 35, 5–22.
Fajardo, A.R., Lopes, L.C., Rubira, A.F., Muniz, E.C., 2012. Development and application of chitosan/poly(vinyl alcohol) films for removal and recovery of Pb(II). Chem. Eng. J. 183, 253–260.
Furusawa, T., Smith, J.M., 1973. Fluid-particle and intraparticle mass transport rates in slurries. Ind. Eng. Chem. Fundam. 12, 197–203.
Goldstein, J.I., Newbury, D.E., Echil, P., Joy, D.C., Romig Jr., A.D., Lyman, C.E., Fiori, C., Lifshin, E., 1992. Scanning Electron Microscopy and X-ray Microanalysis. Plenum Press, New York.
Gupta, V.K., Ali, I., 2013. Environmental Water Advances in Treatment, Remediation and Recycling. Elsevier, Amsterdam.
Gupta, V.K., Suhas, 2009. Application of low-cost adsorbents for dye removal: a review. J. Environ. Manage. 90, 2313–2342.
Hessel, C., Allegre, C., Maisseu, M., Charbit, F., Moulin, P., 2007. Guidelines and legislation for dye house effluents. J. Environ. Manage. 83, 171–180.
Koprivanac, N., Kusic, H., 2008. Hazardous Organic Pollutants in Colored Wastewaters. New Science Publishers, New York.
Kyzas, G.Z., Lazaridis, N.K., 2009. Reactive and basic dyes removal by sorption onto chitosan derivatives. J. Colloid Interface Sci. 331, 32–39.
Lee, V.K.C., McKay, G., 2004. Comparison of solutions for the homogeneous surface diffusion model applied to adsorption systems. Chem. Eng. J. 98, 255–264.
Li, P., Xiu, G., Rodrigues, A.E., 2003. Modeling separation of proteins by inert core adsorbent in a batch adsorber. Chem. Eng. Sci. 58, 3361–3371.
Li, X., Li, Y., Zhang, S., Ye, Z., 2012. Preparation and characterization of new foam adsorbents of poly(vinyl alcohol)/chitosan composites and their removal for dye and heavy metal from aqueous solution. Chem. Eng. J. 183, 88–97.
Mirmohseni, A., Seyed Dorraji, M.S., Figoli, A., Tasselli, F., 2012. Chitosan hollow fibers as effective biosorbent toward dye: preparation and modeling. Bioresour. Technol. 121, 212–220.
Moussavi, G., Khosravi, R., 2011. The removal of cationic dyes from aqueous solutions by adsorption onto pistachio hull waste. Chem. Eng. Res. Des. 89, 2182–2189.
Ocampo-Perez, R., Leyva-Ramos, R., Alonso-Davila, P., Rivera-Utrilla, J., Sánchez-Polo, M., 2010. Modeling adsorption rate of pyridine onto granular activated carbon. Chem. Eng. J. 165, 133–141.
Ocampo-Perez, R., Leyva-Ramos, R., Mendoza-Barron, J., Guerrero-Coronado, R.M., 2011. Adsorption rate of phenol from aqueous solution onto organobentonite: surface diffusion and kinetic models. J. Colloid Interface Sci. 364, 195–204.
Ocampo-Pérez, R., Rivera-Utrilla, J., Gómez-Pacheco, C., Sánchez-Polo, M., López-Peñalver, J.J., 2012. Kinetic study of tetracycline adsorption on sludge-derived adsorbents in aqueous phase. Chem. Eng. J. 213, 88–96.
Piccin, J.S., Dotto, G.L., Vieira, M.L.G., Pinto, L.A.A., 2011. Kinetics and mechanism of the food dye FD&C red 40 adsorption onto chitosan. J. Chem. Eng. Data 56, 3759–3765.
Qiu, H., Pan, L.L., Zhang, Q.J., Zhang, W., Zhang, Q., 2009. Critical review in adsorption kinetic models. J. Zhejiang Univ. Sci. A 10, 716–724.
Ruthven, D.M., 1984. Principles of Adsorption and Adsorption Processes. John Wiley & Sons, New York.
Saratale, R.G., Saratale, G.D., Chang, J.S., Govindwar, S.P., 2011. Bacterial decolorization and degradation of azo dyes: a review. J. Taiwan Inst. Chem. Eng. 42, 138–157.
Srinivasan, A., Viraraghavan, T., 2010. Decolorization of dye wastewaters by biosorbents: a review. J. Environ. Manage. 91, 1915–1929.
Strauss, W.A., 2008. Partial Differential Equations: An Introduction. John Wiley & Sons, New York.
Suzuki, M., 1990. Adsorption Engineering. Kodansha, Tokyo.
Valderrama, C., Gamisans, X., de las Heras, X., Farrán, A.M., Cortina, J.L., 2008. Sorption kinetics of polycyclic aromatic hydrocarbons removal using granular activated carbon: intraparticle diffusion coefficients. J. Hazard. Mater. 157, 386–396.
Verma, A.K., Dash, R.R., Bhunia, P.A., 2012. A review on chemical coagulation/flocculation technologies for removal of colour from textile wastewaters. J. Environ. Manage. 93, 154–168.
Wan Ngah, W.S., Teong, L.C., Hanafiah, M.A.K.M., 2011. Adsorption of dyes and heavy metal ions by chitosan composites: a review. Carbohydr. Polym. 83, 1446–1456.
Weber Jr., W.J., Di Giano, F.A., 1995. Process Dynamics in Environmental Systems. John Wiley & Sons, New York.
Wegmann, C., Suárez-García, E., Kerkhof, P.J.A.M., 2011. Kinetics of acrylonitrile adsorption from an aqueous solution using Dowex Optipore L-493. Sep. Purif. Technol. 81, 429–434.
Weska, R.F., Moura, J.M., Batista, L.M., Rizzi, J., Pinto, L.A.A., 2007. Optimization of deacetylation in the production of chitosan from shrimp wastes: use of response surface methodology. J. Food Eng. 80, 749–753.
Wilke, C.R., Chang, P., 1955. Correlation of diffusion coefficients in dilute solutions. AIChE J. 1, 264–268.
Zhu, H.Y., Fu, Y.Q., Jiang, R., Yao, J., Xiao, L., Zeng, G.M., 2012. Novel magnetic chitosan/poly(vinyl alcohol) hydrogel beads: preparation, characterization and application for adsorption of dye from aqueous solution. Bioresour. Technol. 105, 24–30.

Please cite this article in press as: Dotto, G.L., et al., Diffusional mass transfer model for the adsorption of food dyes on chitosan films. Chem. Eng. Res. Des. (2014), http://dx.doi.org/10.1016/j.cherd.2014.03.013